MECHANISMS AND PREVENTION OF SCALE FORMATION IN BOILERS

M. Jamialahmadi

The University of Petroleum Industry
Ahwaz, Iran

H. Muller-Steinhagen

Department of Chemical and Process Engineering
The University of Surrey
Surrey, England

Abstract Nucleate boiling heat transfer coefficients may be strongly reduced by scale formation, even for conditions where the bulk foulant concentration is well below the saturation concentration. Due to the mechanism of micro-layer evaporation, the local concentration at the heat transfer surface can be considerably increased, causing the formation of scale and changes in bubble frequency and bubble departure diameter. The interaction between scale formation and bubble formation is studied with a precision pool boiling test apparatus in conjunction with a microprocessor-controlled camera and video equipment. The effects of EDTA which is commonly used as an antifouling agent in industrial boilers, on saturated pool boiling in the presence of foulants are discussed.

Key Words Boiling, Fouling, Bubble, Nucleation, EDTA

چکیده دیگهای بخار بطور گسترده در پالایشگاهها، مجتمع های شیمیائی و پتروشیمیائی و نیروگاههای حرارتی مورد استفاده قرار می گیرند. یکی از پدیده هائی که هنوز در دیگهای بخار کاملا شناخته نشده است تشکیل رسوب ناخواسته مواد معلق یا محلول در سیال برروی سطوح انتقال حرارت دیگها می باشد که باعث کاهش شدید ضریب انتقال حرارت سیستم می گردد. دراین مقاله مکانیسم تشکیل رسوب سولفات کلسیم در جوشش حوضچه ای از طریق اندازه گیری ضریب کلی انتقال حرارت، اندازه حبابها و توزیع محلهای حباب خیز مورد مطالعه قرار گرفته است. طبیعت رسوبهای تشکیل شده برروی سطح انتقال حرارت در جریانهای حرارتی مختلف نیز با استفاده از Scan Microscopy مورد مطالعه قرار گرفته و تأثیر EDTA که بعنوان ضد رسوب در دیگهای بخار استفاده می شود برروی میزان تشکیل رسوب نیز بررسی شده است

INTRODUCTION

Intensive studies, both experimental and theoretical, have been performed over the past decades on nucleate boiling heat transfer which have been reviewed recently by Nishikawa and Fujita [1]. Sharply rising fuel costs in refineries, chemical and petrochemical plants requires increasing emphasis on energy conservation programs and demands a deeper knowledge of the phenomena related to boiling heat transfer than ever before. One phenomenon which is still not understood is the fouling of the boilers. Fouling deposits pose a barrier to heat transfer which means additional energy is required to maintain desired process conditions. Eventually, operations must be curtailed to remove these deposits, which results in high heat exchanger cleaning and downtime costs.

A review of the existing literature on the mechanisms of boiler scale formation reveals that there have been few serious attempts to understand the effects of boiling mechanisms on the formation of scale. Experimental results are scarce and incomplete and have been summarized by Palen [2] and Palethorpe [3].

Steam generation rates per square meter of heat transfer surface are far greater for today's units than they were 10 to 20 years ago. This implies that the wall superheat has been greatly increased in modern boilers, which in turn,

requires improved treatment programs. This trend has led to the common use of solubilizing treatments employing chelates. Many chelating agents are available commercially, but the one which has found widespread application for boiler deposit control is disodium salt of ethylenediaminetetraacetic acid known as EDTA. The effect of this compound on the boiling heat transfer coefficient in the presence of fouling is still unknown. It is necessary to understand the effect of this compound on the boiling mechanism before the proper selection of an antifoulant can be made.

The main objective of this work is to study systematically the mechanism of fouling in pool boiling in the absence and presence of antifoulant EDTA by measuring overall heat transfer coefficient, bubble size, bubble frequency and nucleation site distribution during the fouling period.

EXPERIMENTAL EQUIPMENT AND PROCEDURE

The pool boiling apparatus shown in Figure 1 was used for the present investigation. It consists of a thick-walled cylindrical stainless-steel tank containing approximately 30 litres of test liquor and of a vertical condenser to condense and recycle the evaporated liquid. The test heater is mounted horizontally within the tank and can be observed and photographed through observation glasses. The temperature in the tank is regulated by an electronic temperature controller and a variac in conjunction with two band heaters convering the complete cylindrical outside surface. Boiling occurs at the smooth outside of an electrically-heated cylindrical stainless-steel heater with 10.7 mm diameter. Four thermocouples are embedded in the wall close to the heat transfer surface. The liquid bulk temperature was measured with a platinum resistance thermometer. Test equipment, data acquisition, data reduction and experimental procedure are described in more detail elsewhere [4].

Initially, the test heater and tank were cleaned, the

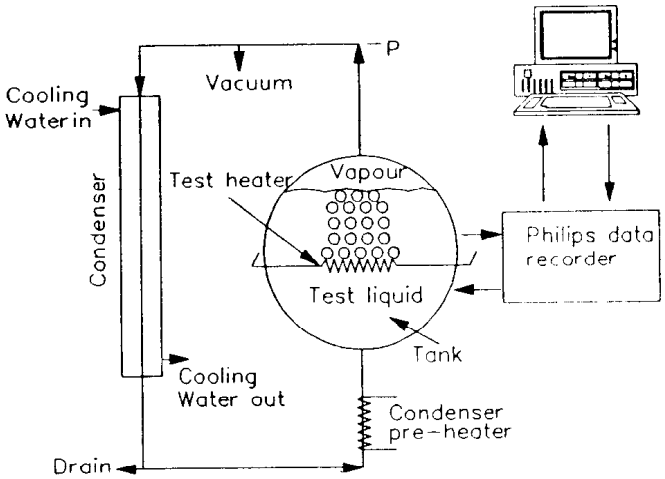

Figure 1. Schematic diagram of pool boiling apparatus

observation windows closed, and the system was connected to the vacuum pump. Once the pressure of the system reached approximately 0.1 bar, the salt solution (prepared 24 hours earlier) was introduced. Following this, the tank heater and condenser preheater were switched on and the temperature of the system was allowed to rise to the saturation temperature. Meanwhile, the system was de-aerated several times and then left at saturation temperature and atmospheric pressure for about five hours to obtain a homogeneous condition throughout the system. Then, the power was supplied to the test heater and kept at a predetermined value. The data acquisition system, microprocessor-controlled camera and video equipment were simultaneously switched on to record temperatures, pressure, heat flux, bubble departure diameter and bubble frequency.

Immediately, after the run, the solution was drained and the test heater was allowed to cool and dry. It was removed from the system and a sample from the deposition was taken for electron scanning microscopy.

RESULTS AND DISCUSSIONS

Most models used to describe nucleate boiling are based on the hypothesis that nucleate boiling is a local phenomenon and that the bubble behaviour near the heating surface has a dominant effect on heat transfer. One such model

recently presented by Jamialahmadi *et al.* [5] is:

$$\alpha = n\pi d_b^2 (\alpha_b - \alpha_c) + \alpha_c \qquad (1)$$

where

$$\alpha_b = \frac{2}{\sqrt{\pi}} \sqrt{\lambda_L \rho_L C_p} \sqrt{f} + \frac{\rho_L \Delta h_v f d_b}{6 \Delta T} \qquad (2)$$

According to Frite [6] the bubble diameter is given by:

$$d_b = 0.0146\beta \left[\frac{2\sigma}{g(\rho_L - \rho_v)}\right]^{0.5} \qquad (3)$$

Equations 1 to 3 illustrate the importance of bubble diameter, bubble frequency and density of nucleation sites on the nucleate boiling heat transfer coefficient. Therefore, it is necessary to understand the effect of fouling deposit (in the absence or presence of EDTA) on these parameters before a physically sound prediction model for the deposition process can be developed.

Calcium Sulphate Deposition in the Absence of EDTA

Heat transfer coefficient

The experiments were carried out in arbitrary sequence. Some runs were repeated to check the reproducibility of the experiments, which proved to be very good, as demonstrated in Figure 2. Figure 3 shows heat transfer coefficients as a function of time for a heat flux of 38522 W/m^2. The general shape of the curve is characterized by a sharp decrease to a minimum (region 1), followed by an increase to a maximum (region 2) and a subsequent gradual decrease towards an asymptotic value (region 3). However, the extent of the variations in heat transfer coefficient with time is strongly affected by the value of the heat flux and the foulant concentration.

The following data were obtained based on observations of the number of active nucleation sites, bubble shape, bubble size and bubble detachment frequency which were made from high speed photographs and several recorded video movies.

Figure 4 shows how the active nucleation sites changed

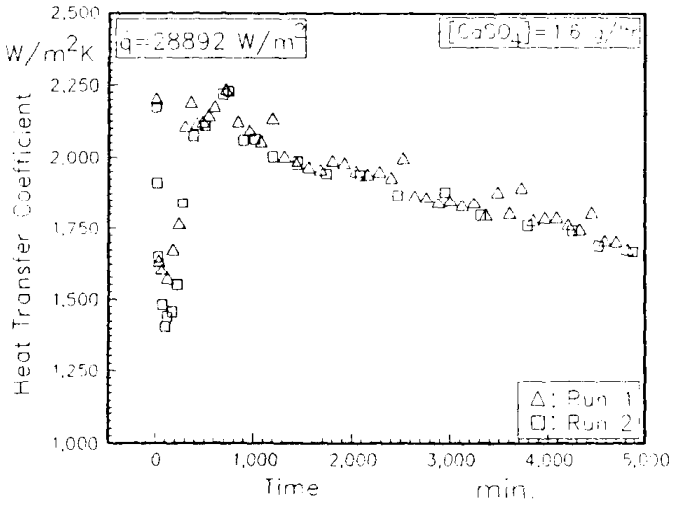

Figure 2. Heat transfer coefficient as a function of time for two experiments with identical conditions

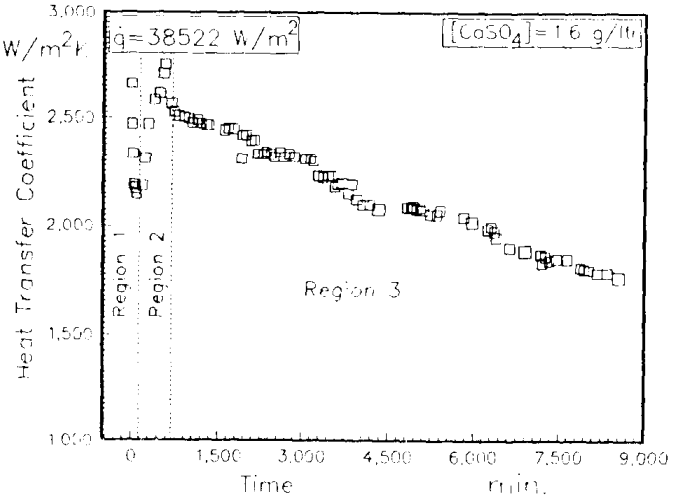

Figure 3. Heat transfer coefficient as a function of time

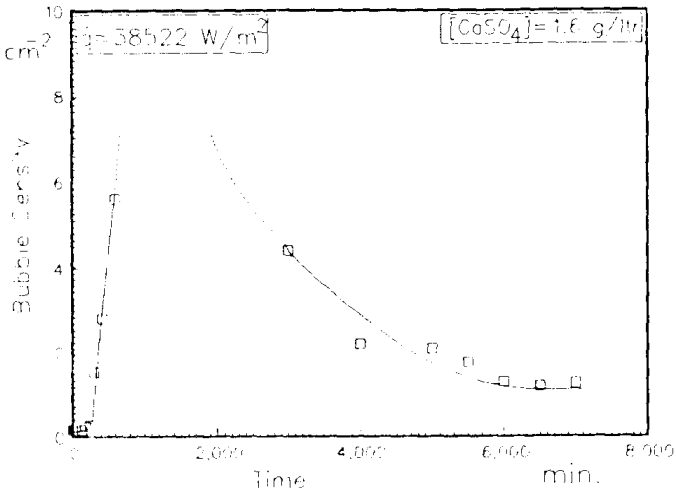

Figure 4. Nucleation site density as a function of time

with time for the above fouling run. Generally, the number of active nucleation sites increases with increasing heat flux. However, there is also a strong effect of operating time on bubble site density. The number of active nucleation sites rises towards a maximum value after which it falls back to a value close to that held at the beginning of the experiment. When comparing these results with the results shown in Figure 3, consistent trends are found. In region 1 only a few nucleation sites were present on the surface of the heating element. The bubbles were hemispherical with an average departure diameter between 1 cm and 2 cm and a frequency of about 7 bubbles per second. In region 2, the number of active nucleation sites increased sharply with time, probably due to the formation of additional sites by the deposit. The number of these sites gradually decreased throughout region 3. In region 2 and 3 only spherical bubbles with departure diameter of about 2 mm were observed. The bubble frequency in these two regions was very high, which made it difficult to distinguish consecutive bubbles.

Effect of deposition on boiling mechanism

As the supersaturation due to the temperature gradient near the heat transfer surface is considerably lower than the supersaturation due to evaporation of the microlayer between bubble and heat transfer surface, the growth rate of deposit in the vicinity of the nucleation sites exceeds that in areas where only natural convection heat transfer occurs. The deposit under the bubbles has a fairly high density and adherence. It restricts the formation of further bubbles, thus causing the sharp drop in heat transfer as observed for region 1. After a certain length of time, the slow-growing, porous deposit at the heat transfer surface previously unaffected by bubbles starts to provide additional active nucleation sites, thus increasing the heat transfer coefficient in region 2. Over the following period of time, the combined bubbling/deposition process gradually increases the density of the deposit, de-activating the larger nucleation sites and closing 'steam chimneys', which have been described by MacBeth [7]. Furthermore, the thickness of the deposit increases. This combined process cause the reduction of heat transfer coefficient in region 3.

Effect of $CaSO_4$ concentration

The effect of $CaSO_4$ concentration on the formation of deposits is shown in Figure 5. Both the saturated 1.6 g/l solution and the subsaturated 1.2 g/l solution form deposits. It would seem as if the fouling curves for these two concentrations are approaching a common asymptotic heat transfer coefficient. It is important to note that the 1.2 g/l solution is not saturated with respect to $CaSO_4.1/2H_2O$, even for the wall temperatures at this heat flux. The supersaturation necessary for crystal nucleation and growth must, therefore, be created locally by the bubble growth mechanisms. Hardly any reduction in heat transfer was observed for the 0.8 g/l solution. Two possible conclusions may be drawn from this observation:

1) The concentration effect in the microlayer is less than the reported value of 4-5 orders of magnitude [8].
2) Any deposits re-dissolve rapidly into the bulk liquid because of the high level of turbulence created by the departure of the bubbles from the heat transfer surface.

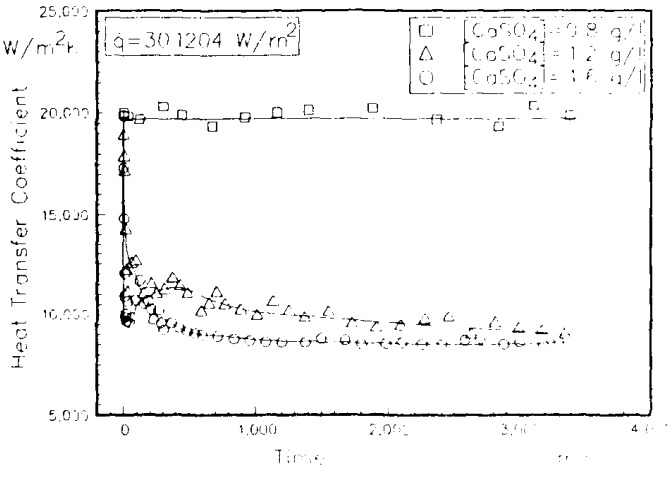

Figure 5. Effect of $CaSO_4$ concentration on the transient reduction of heat transfer coefficient

Nature of deposit

The solubility curve in Figure 6 indicates that the calcium sulphate crystals formed on the heating element should consist of pure anhydride. The appearance of the deposit formed for different heat fluxes varied, as seen from the photographs shown in Figure 7. A short, needle-like structure is characteristic of the deposit formed at low heat flux. With increasing heat flux, the crystals become shorter, harder and more adherent. The thickness and density of the deposit could be measured after each run. The thermal conductivity was found for a given deposit by reducing the heat flux well into the natural convection region and comparing the heat transfer coefficients with those measured previously for pure water:

$$\frac{1}{\alpha}-\frac{1}{\alpha_w}=R_f=\frac{S_d}{\lambda_d}$$

The average density and thermal conductivity of the observed fouling layers is 2040 kg/m^3 and 1.39 W/m.K respectively. These values agree well with the values reported by Krause [10], even though they were obtained under forced convective conditions.

EFFECT OF EDTA CONCENTRATION ON SCALING RATES

Antifoulants are being used successfully by refineries and chemical plants as an effective method for controlling fouling in a variety of process equipment such as reboilers. When fuel was cheap, antifoulants were used mainly for cases of severe fouling where maintenance cost and capacity credits provided the major economic incentives. However, escalating fuel costs and added emphasis on reducing process energy requirements have expanded the range of economic applications to include more moderate fouling streams. Here antifoulants which are injected into the fouling stream have provided a fast solution requiring only low capital investment.

Figure 8 shows heat transfer coefficients as a function of time for heat flux of 301204 W/m^2 and different EDTA

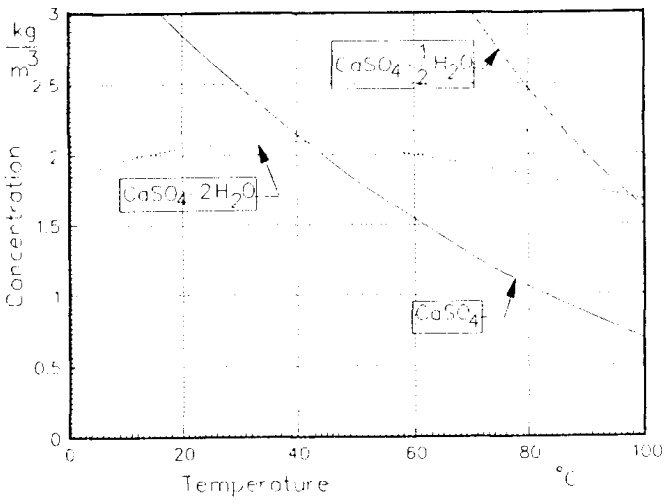

Figure 6. Solubility curve for $CaSO_4$ in water [9]

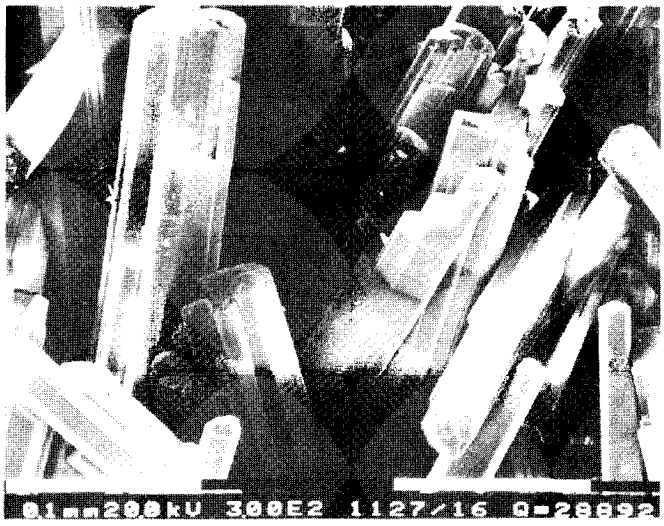

Figure 7. Deposits observed for two different heat fluxes (28892 W/m^2 and 38522 W/m^2)

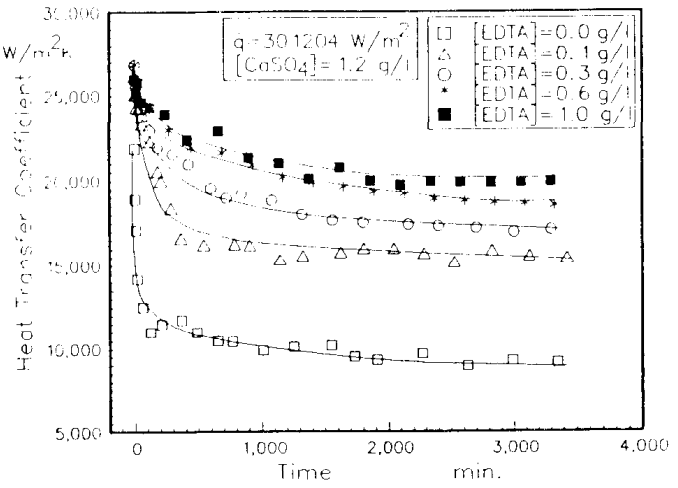

Figure 8. Heat transfer coefficient as a function of time for various EDTA concentrations

concentrations. It illustrates when EDTA is added to the $CaSO_4$ solution, the amount of scale formed on the surface of heating element decreased considerably.

During fouling experiments in the absence of EDTA, bubbles leave behind a ring of deposit when detaching from the nucleation site. Subsequent bubbles build up a disk-shaped deposit from this original ring. This deposit grows and merges with other nucleation sites until the surface is completely covered by deposit. When EDTA is added to the $CaSO_4$ solution, the amount of scale formed on the surface of the heating element decreased considerably. Under no circumstances was the surface fully covered by the scale. Only for the highest heat flux, a small number of very tiny and hard spots of deposit were observed on the heating surface which could subsequently be removed by acid wash.

The usefulness of EDTA as a antifoulant chelate is due to the presence of four or six atoms which are available for co-ordination to metal cations like Ca^{+2}. For the sake of simplicity the disodium salt of EDTA is generally assigned the formula Na_2H_2Y [11] and its reaction with Ca^{+2} may be written as:

$$Ca^{+2} + H_2Y^{-2} \rightarrow CaY^{-2} + 2H^{+} \qquad (5)$$

Therefore, when the EDTA is added to the $CaSO_4$ solution, it sequesters the Ca^{+2} ions. Consequently the driving force for $CaSO_4$ scale is reduced. As Equation 5 shows, a decreasing pH will reduce the concentration of the complexing species, hence EDTA best forms complexes with Ca^{+2} in a basic solution. In the present investigation, the EDTA concentration was varied from 0.1 g/l to 1g/l, which corresponds to 0.034 to 0.34 mol EDTA per mol $CaSO_4$. If about 1/3 of the Ca^{+2} ions are sequestered by the addition of 1 g/l EDTA, the remaining $CaSO_4$ concentration is 0.8 g/l. The observation that this concentration did not produce any notable deposition corresponds well with the results shown in Figure 8.

CONCLUSIONS

The fouling process observed during nucleate boiling of $CaSO_4$ solutions can be divided into three distinct time regions during which different phenomena dominate boiling and deposition. These phenomena can be explained by considering the effect of dissolved and deposited $CaSO_4$. Two different types of deposit have been observed depending on the mechanisms of heat transfer. The major contribution towards the deposition occurs due to the evaporation at the base of growing bubbles. Therefore, the deposition rates increase with an increasing number of nucleation sites.

The scale formation during nucleate boiling of $CaSO_4$ solutions decreased strongly with increasing EDTA addition. Hardly any deposit was observed at high EDTA concentration.

NOMENCLATURE

c_p	specific heat capacity, J/kg.K
d_b	bubble diameter, m
f	bubble frequency, s^{-1}
g	acceleration due to gravity, m/s^2
n	nucleation site density, m^{-2}
R_f	fouling resistance, m^2K/W
S_d	deposit thickness, m
α	heat transfer coefficient, $W/m^2.K$
β	contact angle, degree

Δh_v latent heat of evaporation, J/kg

ΔT temperature difference, K

λ thermal conductivity, W/m.K

ρ density, kg/m^3

σ surface tension, N/m^2

Subscript

b boiling

c natural convection

d deposit

L liquid

V vapour

w water

REFERENCES

1. K. Nishikawa and Y. Fujita: Nucleate boiling heat transfer and its augmentation, *Advances in Heat Transfer*, Vol. 20, pp. 1-79, (1990).
2. J.W. Palen: Fouling of heat transfer surfaces, M.Sc. Thesis, Univ. Illinois, Urbana, (1965).
3. S.J. Palethorpe and J. Bridgewater: The influence of surface finish on calcium sulphate fouling, Int. conf. on Foluing in Process Plant, Oxford, pp. 355-372, (1988).
4. M. Jamialahmadi and H. Muller-Steinhagen: Pool boiling heat transfer to electrolyte solutions, *Chem. Eng. Process*, Vol 28, pp. 79-88, (1990).
5. M. Jamialahmadi, R. Blochl and H. Muller-Steinhagen: Pool boiling heat transfer to saturated water and refrigerant 113, *Can. J. Chem. Eng.*, Vol. 64, pp. 746-754, (1990).
6. W. Fritz: Maximum volume of vapour bubbles, *Phys.*, Vol. 36, pp. 379-384, (1935).
7. R.V. MacBeth: Boiling on surfaces overlayed with a porous deposit: Heat transfer rates obtainable by capillary action, AEEW-711, (1971).
8. Heat Transfer and Fluid Flow Services (Harwell U.K.), Seminar on Heat Exchanger Fouling, New Orleans, (1986).
9. Landolt-Bornstein: *"Zahlenwerte und Funktionen,"* Vol.2, Sect.b, Springer-Verlag, Berlin, (1985).
10. S. Krause: Fouling an Warmeubertragungsfachen durch Kristallisation und Sedimentbildung, VDI-Forschungsh., pp. 637-640.
11. A.T. Vogel: *"A Text-Book of Quantitative Inorganic Analysis,"* 3rd ed., Longmans, London, (1961).